A Spherical Source Model for the Thermal Pulse Decay Method of Measuring Blood Perfusion: A Sensitivity Analysis

C. J. Diederich
Radiation Oncology Department,
Arizona Health Science Center,
Tucson, Az. 85724; also,
Electrical and Computer Engineering
Department,
University of Arizona, Tucson, Az. 85721

S. Clegg

R. B. Roemer
Radiation Oncology Department,
Arizona Health Science Center,
Tucson, Az.; also,
Aerospace and Mechanical Engineering
Department,
University of Arizona,
Tucson, Az. 85721

The thermal pulse-decay method, as developed and analyzed by Chen et al. [1-6], is a thermal clearance technique that uses a small thermistor probe for determining the blood perfusion and thermal conductivity of the tissue immediately surrounding the probe. They described the energy transfer of the probe/tissue system mathematically with a simple analytical model, the point source model, which assumes that the heating source is infinitely small. This paper introduces a new, more accurate analytical description that assumes the heating source is spherically symmetric with a finite radius. A numerical study of these two alternative mathematical models is presented in which the solutions of each model are compared to transient temperature decay data generated from a detailed finite difference simulation of the probe/tissue system. The accuracy and sensitivity of the predictions of each of these models to variations in tissue thermal conductivity and perfusion, probe characteristics, and heating time are presented. In all cases, the accuracy of the spherical source model was better than the point source model. It is also shown that the spherical source model can accurately predict low rates of perfusion (on the order of 1 kg/m³s) unlike the point source model. The spherical source model also allows for the possibility of the measurement probes to be calibrated for an "effective bead radius" which accounts for the nonideal characteristics of the probe, thereby giving even more accurate determinations of perfusion.

Introduction

Knowledge of the thermo-physical and related physiological properties of biological materials is critical to the accurate thermal modeling of tissue. The blood perfusion is considered the most important property in determining the temperature distributions, particularly during hyperthermia treatments [7]. The ability to measure and map tumor and normal blood flow, both before and during a hyperthermia treatment, could improve the accuracy of the treatment modeling and estimation of the temperature field and thereby provide for a more effective treatment. There are numerous methods now in use to determine the blood perfusion to various organs and regions of tissue such as tumors. A summary of indicator and thermal clearance techniques has been presented by Eberhart et al. [8], while an overall review of measurements of the thermal properties of biological materials has recently been presented by Chato [9].

This paper will consider a thermal clearance technique, known as the thermal pulse-decay method, for determining the blood perfusion and thermal conductivity in tissues [1-6]. This method utilizes a small invasive thermistor probe which is subjected to a short pulse of power. The subsequent temperature decay is then measured and curve fit to an analytical model to yield the estimates of thermal conductivity and blood perfusion. The original thermal pulse decay probe was described by Goldenberg [10]. Chen et al. [1] improved the model by using "small" thermistor probes. They assumed that the probe is a point source because of its "small" size and derived an analytical description of the temperature decay based on this point source model (PSM). Theoretical studies of the point source model have been performed by Arkin et al. [5-6]. The theoretical assumptions of the point source model were justified by Arkin's analysis where the effects of bead radius, nonhomogeneity of the surrounding tissue region, and tissue trauma were shown to be negligible during the optimal measurement time interval [5]. Also, the effects of experimentally derived errors (those errors propagated from errors in the measurement data) on the overall error in the calculated values of perfusion and thermal conductivity were determined. From these studies an ideal experimental protocol was established that limited the effects of the experimental and theoretical errors on the parameter estimations. The optimal measurement protocol was shown to be dependent on the actual values of tissue perfusion and thermal conductivity, and at low and moderate simulated perfusion rates the dominant error was in the prediction of perfusion.

From the above work it is apparent that the thermal pulse

Contributed by the Bioengineering Division for publication in the JOURNAL OF BIOMECHANICAL ENGINEERING. Manuscript received by the Bioengineering Division, April 19, 1988; revised manuscript received December 12, 1988.

decay method is a worthwhile approach to measuring blood perfusion. It is also apparent that the point source model is only an approximation of the actual thermobead/tissue system. The purpose of this paper is twofold; to introduce an improved model of the TPD system, the spherical source model (SSM), and to extend the theoretical work of Arkin by comparing this model's error with those of the point source model (PSM) under various simulated experimental conditions [11]. Also, the ability of these models to predict low values of blood perfusion is investigated.

At this point it should be noted that these solutions for the thermal pulse-decay method are derived from the bio-heat transfer equation (BHTE). The BHTE is an approximate representation of the heat transfer process in the tissue. Nonetheless, due to its solvability, most thermal techniques for determining tissue properties utilize the BHTE to obtain their solutions. The accuracy of the BHTE and a comparison to other existing tissue models can be found in the survey by Roemer [12].

Methods

Physical Description of Thermobead/Tissue System. The actual physical configuration of the TPD system consists of a thermistor probe imbedded within the tissue region of interest. In experimental and clinical applications of this technique, the thermistor bead is mounted to the tip of a rigid probe assembly and coated with a layer of epoxy [4]. The thermistor bead (Fig. 1) consists of an inner, solid prolate spheroid composed of a resistive composite material, surrounded by successive annular coatings of glass and epoxy. The power is generated electrically within the resistive region. The passive coatings and the composite material of the bead each possess different thermal properties. The thermistor is thus a nonuniform power source with finite dimensions and distinct, inhomogeneous material properties. The tissue that surrounds the probe has separate thermal properties from those of the probe and may have a nonhomogeneous distribution of these properties within the tissue region itself. Also, the effects of trauma due to the insertion of the probe can result in different thermal parameters for the damaged region other than those of the nondamaged tissue region.

Description/Derivation of Analytical Models. The point source model, as developed by Chen et al. [1], is an approximate solution to the above system in that it assumes that the probe is an infinitely small power source (a point source) surrounded by an infinite, homogeneous tissue region. This representation does not account for the finite size and inhomogeneous composition of the thermobead as a power source and as a temperature sensing device. The assumption of an infinite media is valid as long as the tissue is homogeneous over a volume greater than the effective measurement volume sensed by the probe.

The new spherical source model (SSM) more accurately describes the thermistor probe by accounting for the finite size of the heated volume of the thermobead. It does this by using a spherical power distribution with the same diameter as the thermistor. Otherwise, the SSM makes the same assumptions as the PSM, including homogeneity of all tissue parameters throughout an infinite region, including the thermistor. Neither model takes into account the separate thermal properties of the bead.

The derivations of both the spherical and point source analytical models assume that the bio-heat transfer equation adequately describes the thermal processes in the surrounding tissue region. (Note that the BHTE is an approximate representation of the heat transfer processes in tissue. Therefore, the term W is an approximation of the true tissue perfusion.) Thus, the equation describing the behavior of the point source model system can be written as:

$$\rho_t c_t \frac{\partial \Theta_t}{\partial t} = k_t \nabla^2 \Theta_t - W c_{bl} \Theta_t + Q_b \delta(0,t) \tag{1}$$

where Θ_t is the temperature above the steady state temperature field, thus the boundary and initial conditions for equation (1) are zero. However, in the spherical source analysis it is assumed that the power applied to the bead (Q_b) is of finite extent and is uniformly distributed in a sphere with a radius equal to the outer bead radius, R. Using the same assumptions implicit in equation (1), the equation for the spherical source model reduces to the following, where H is the Heavyside function:

$$\rho_t c_t \frac{\partial \Theta_t}{\partial t} = k_t \nabla^2 \Theta_t - W c_{bl} \Theta_t + Q_b [1 - \mathrm{H}(\bar{r} - R)] \tag{2}$$

As in equation (1), the initial and boundary conditions for this equation are zero. A Green's function analysis can be used to solve equations (1) and (2), for the temperature at $r = 0$:

$$\text{(PSM)} \quad \Theta_p(0,t) = \gamma \left(\frac{\alpha}{2\pi}\right)^{3/2} \int_0^\tau (t-s) e^{-\beta(t-s)} ds \tag{3}$$

or

$$\text{(SSM)} \quad \Theta_s(0,t) = \gamma \int_0^\tau e^{-\beta(t-s)} \left\{ \mathrm{erf}\left(\frac{R}{\sqrt{4\alpha(t-s)}}\right) - \frac{R}{\sqrt{\pi\alpha(t-s)}} e^{-R^2/4\alpha(t-s)} \right\} ds \tag{4}$$

where

$$\alpha = \frac{k}{\rho c_t}$$

$$\beta = \frac{W c_{bl}}{\rho c_t}$$

$$\gamma = \frac{Q_b}{\rho c_t}$$

Equations (3) and (4) represent the point source model (PSM) as derived by Chen et al. [1] and the spherical source model (SSM), respectively, where $\Theta(t)$ is the temperature measured

Nomenclature

c = specific heat, J/kg°C
k = thermal conductivity, W/m°C
t = time, s
Q = volumetric power, W/m^3
P = power, W
R = outer bead radius, m
T = temperature, °C
W = perfusion, kg/m^{3}s
D = domain of influence
ρ = density, kg/m^3
Θ = $T(r,t) - T(r,0)$ = temperature above the initial temperature, °C
τ = power pulse length, s
t_m = central measurement time, s
δ = dirac delta function

Subscripts

ar = arterial
b = thermistor bead
bl = blood
p = point source
s = spherical source
t = tissue
rm = reference model parameter
am = analytical model parameter

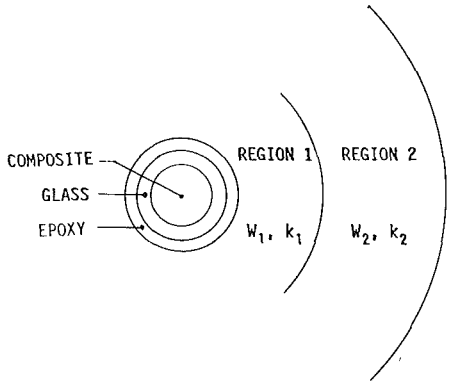

Fig. 1 Physical configuration of the finite difference reference model showing the TPD probe and surrounding regions

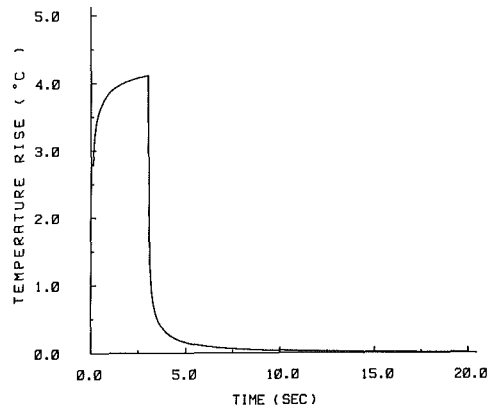

Fig. 2 Typical simulated temperature decay curve produced from the reference model. Parameters used: $W = 10$ kg/m^{3}s, $k = 0.5$ W/m°C, $\tau = 3$ seconds, $P = 5$ mW.

by the thermistor above the steady state temperature. Since both equations (3) and (4) are integral equations which do not yield simple elementary functions when directly integrated, they were solved numerically using the Romberg method [13].

Reference Model Description. In order to generate a data base which could be used to systematically evaluate the accuracy of the two analytical models, a reference model was developed which more accurately describes the actual probe geometry. A finite difference representation of the geometry of Fig. 1 was developed in spherical coordinates with variable thermal properties, using a fully implicit tridiagonal solver to calculate the one dimensional, transient temperature distributions.

The reference model allows for regions of different thermal properties in the thermobead and the surrounding tissues. The resistive composite was modeled as a spherical power source and temperature sensing element of a specified radius, surrounded by passive coatings of glass and epoxy. These three regions have separate thermal conductivities and no perfusion. The tissue medium was modeled as a series of concentric spherical regions surrounding the thermistor bead. The number, size, and thermal properties of these concentric regions could be varied according to the desired simulation design. Only one annular region of tissue medium was modeled for most of the conditions simulated. The outer spherical boundary of the tissue media was set at a radius of 2 cm, which was sufficient for all of the analysis since the temperature gradients near the boundary were negligible for all cases.

The temperatures calculated from this reference model are considered to be a more accurate representation of the actual probe response than are the temperatures from either analytical model because the thermistor was more accurately modeled. Thus, the reference model temperatures were used as a common basis of comparison for the predictions of the two analytical models. The comparison was performed by generating a set of power-off transient temperature data from the reference model for a given set of conditions (thermal conductivity and blood perfusion). This transient data was then used as if it were actual temperature data measured by a probe. The two analytical models were then fit to that "experimental data" to predict the local tissue perfusion and thermal conductivity. The accuracy of those predictions were then compared to the known tissue properties (i.e., those of the reference model that were used to generate the "experimental data").

Reference Model Simulations

The standard reference model was chosen to have an outer diameter of 0.3 mm and an inner composite diameter of 0.2 mm to be consistent with the probes used in experimental situations. The average values of the thermal properties of the thermistor bead were taken from the literature and used in the simulations. The thermal conductivity of common nickel-oxide and nickel-magnesium-oxide composites range in value from 2 to 14 W/m°C [14]. For this study, the thermal conductivity of the composite was generally chosen as 10 W/m°C, with a few comparisons made using values of 1 and 14 W/m°C. The outer glass coating was chosen to have a thermal conductivity of 1.4 W/m°C [15]. The layer of epoxy resin was chosen to have a thermal conductivity of 0.21 W/m°C [16]. Some theoretical decay curves were also produced for beads with an outer diameter of 0.4 mm to study the effects of bead diameter on the solutions.

The tissue parameters used to generate data were chosen to generously bracket the expected physiological values. In the parametric studies, the tissue thermal conductivity was varied from 0.3 to 0.7 W/m°C and the local perfusion values ranged from 1 to 50 kg/m^{3}s. The power delivered to the thermistor was 5 mW and the pulse length was varied from 1 to 5 seconds. The simulation parameters as used in most comparisons were as follows: a tissue perfusion of 10 kg/m^{3}s, tissue thermal conductivity of 0.5 W/m°C, and a pulse length of 3 seconds.

To generate the reference model temperature decay data, the finite difference program was run on a VAX 750 using double precision accuracy. To obtain a high degree of accuracy, the finite difference solution used a time step of 0.1 milli-seconds and a grid size of 4 microns throughout all regions. This grid size was chosen to give a high degree of accuracy with as short as possible of a computation time. The transient temperature data were recorded in 0.1 second interval for a total time of 20 seconds. A plot of a typical simulated temperature decay versus measurement time is shown in Fig. 2.

The temperature data from the reference model were then used to evaluate the predictions of perfusion and thermal conductivity obtained from each analytical model (equations (3) and (4)). The radius of the reference model thermistor, including the layer of epoxy, was used as the radius of the heated sphere for the SSM solutions unless noted otherwise. An optimization program was used to determine the perfusion and thermal conductivity of each of the analytical models for every set of reference model transient temperature data. The optimization routine used the Gauss method of parameter estimation [17].

To investigate the accuracy of the model predictions as a function of the time at which the temperature measurements were made, the parameter estimations were computed for an interval of 1.2 seconds, centered at each desired measurement time (t_m). For example, since the temperature data was recorded in 0.1 second increments, the parameter estimations at the central measurement time of 10 seconds were determined by

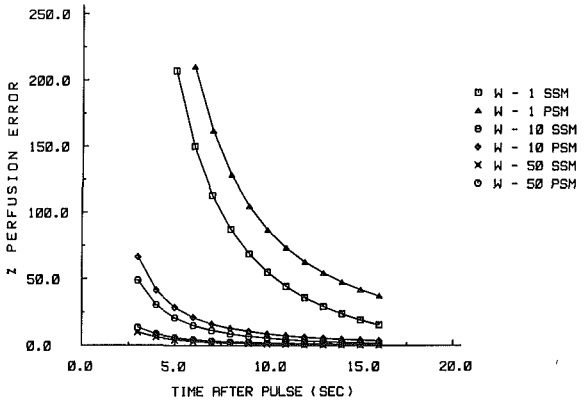

Fig. 3 Perfusion prediction errors for the PSM and SSM versus time after pulse. Parameters used: $k = 0.5$ W/m°C, $\tau = 3$ seconds, $P = 5$ mW. W is varied from 1-50 kg/m^{3}s.

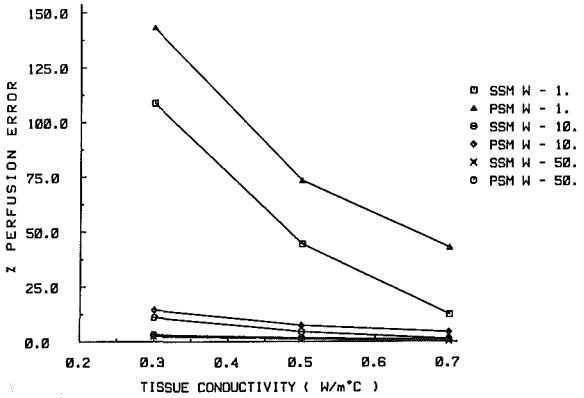

Fig. 4 Effects of the reference model tissue conductivity and perfusion on the perfusion errors of each model for a discrete measurement time (t_m) of 11 seconds after the pulse. Parameters used: $\tau = 3$ seconds, $P = 5$ mW.

using the measured temperature data from 9.4 to 10.6 seconds. The reason for these discrete evaluations was to illustrate how the effects of the inherent model errors varied with measurement time. The errors were computed as the absolute value of the difference between the parameter values predicted by each model and the actual, known values used in the reference model simulation program.

Results

The parameter prediction errors for each of the analytical models for various perfusion rates, tissue thermal conductivities, pulse lengths, and dimensions and thermal properties of the thermistor bead are given in Figs. 3–8. For all of these tests, the parameters were constant as follows, unless noted otherwise; $W_{rm} = 10$ kg/m^{3}s, $k_{rm} = 0.5$ W/m°C, $\tau = 3$ seconds, $R_{rm} = 0.15$ mm, and an applied power of 5 mW. Figure 3 shows the errors in predicting perfusion for each analytical model, the SSM and PSM, as a function of measurement time for several simulated perfusion magnitudes (1, 10, and 50 kg/m^{3}s).

The percent error of each model in predicting perfusion versus the tissue thermal conductivity of the reference model is shown in Fig. 4, where the reference model perfusion was varied between 1, 10, and 50 kg/m^{3}s. The perfusion error of each model was also plotted against the simulated heating pulse length, again as the perfusion was varied, as shown in Fig. 5. The central measurement time (t_m) was 11 seconds after the pulse for all of these determinations.

Figures 6(a) and 6(b) are plots of the error in the perfusion prediction model versus the central measurement time for various dimensions of the reference model thermobead for the

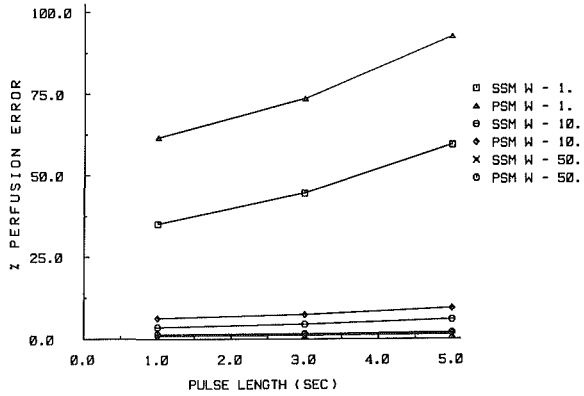

Fig. 5 Effects of pulse length and simulated perfusion on perfusion errors of each model for a discrete measurement time of 11 seconds after the pulse. Parameters used: $k = 0.5$ W/m°C, $P = 5$ mW, τ is varied between 1, 3, and 5 seconds, and W is varied between 1, 10, and 50 kg/m^{3}s. Both SSM and PSM solutions are used.

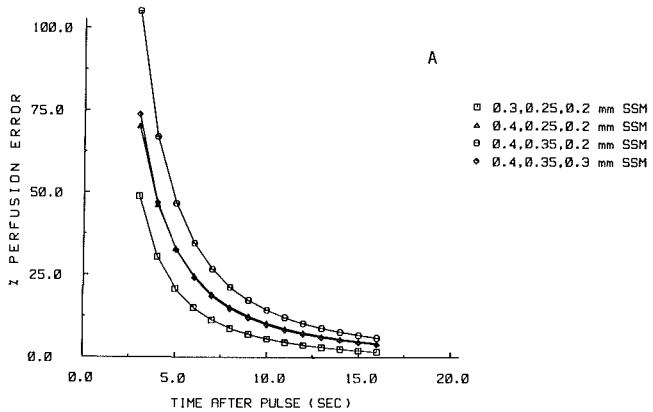

Fig. 6(a)

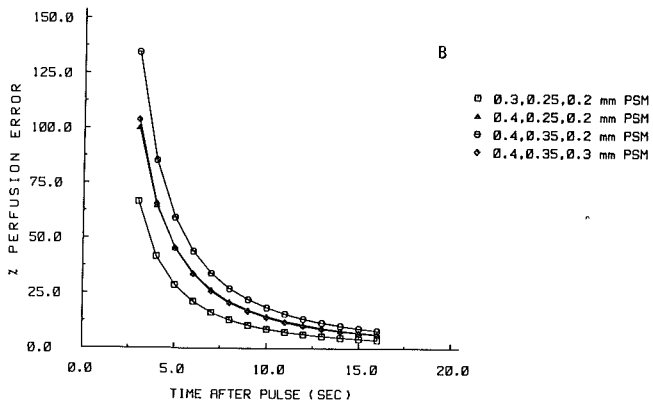

Fig. 6(b)

Fig. 6 Effects of the thermobead dimensions on the perfusion error of the (a) SSM and (b) PSM. Parameters used: $k = 0.5$ W/m°C, $\tau = 3$ seconds, $P = 5$ mW, $W = 10$ kg/m^{3}s. Four different bead geometries were tested. The dimensions given are the outer diameters of the three layers—epoxy, glass, and inner composite.

SSM and PSM, respectively. The inner composite diameter was varied from 0.2 mm to 0.3 mm and the outer bead diameter from 0.3 mm and 0.4 mm. The other experimental values were held constant at the nominal values.

To show the effects of tissue trauma due to needle insertion, the perfusion error of the PSM and SSM model is plotted against the measurement time in Fig. 7 for cases where the thickness of a nonperfused region surrounding the probe is varied from zero to a distance of 0.45 mm (3 bead radii thick).

To study the dependence of the spherical source model

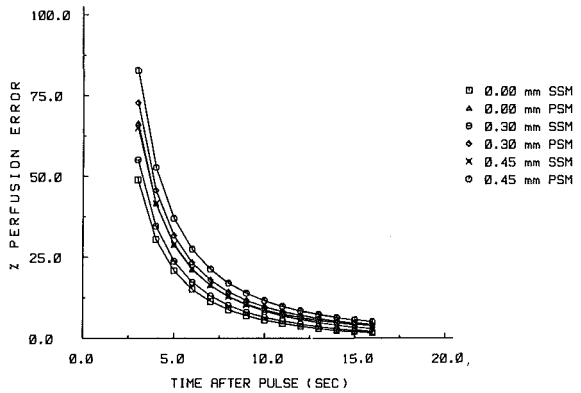

Fig. 7 Effects of traumatized tissue on the perfusion error of the SSM. Parameters used: $k = 0.5$ W/m°C, $\tau = 3$ seconds, $P = 5$ mW, $W = 10$ kg/m^{3}s. The damaged tissue region was modeled as a spherical annulus, with zero perfusion, surrounding the bead. The trauma region was varied from 0.0 mm to 0.45 mm (3 bead radii) from the outer surface of the standard reference model bead.

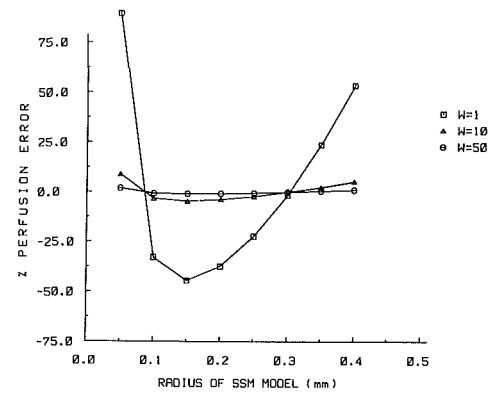

Fig. 8 Effects of different values of the radius (heated region) in the SSM on the subsequent predictions of perfusion. The Reference Model data were obtained with the following parameters; $R_{rm} = 0.15$ mm, $k = 0.5$ W/m°C, $\tau = 3$ s, and the perfusion was varied between 1, 10, and 50 kg/m^{3}s.

prediction on the value of the bead radius (heated region) used to obtain the solutions, the perfusion errors of the SSM for various perfusions (1, 10, and 50 kg/m^{3}s) are plotted in Fig. 8 against the radius (heated region) used in the SSM solution. For these tests, the reference model outer bead radius was 0.15 mm, $k_{rm} = 0.5$ W/m°C, $\tau = 3$ seconds, $P = 5$ mW, and $W_{rm} = 1$, 10, or 50 kg/m^{3}S. Figure 9 is a plot of the SSM perfusion errors as a function of measurement time for several simulated perfusion magnitudes (1, 10, and 50 kg/m^{3}s). In this figure the radius of the heated region in the SSM was 0.3 mm, i.e., twice the reference model bead radius.

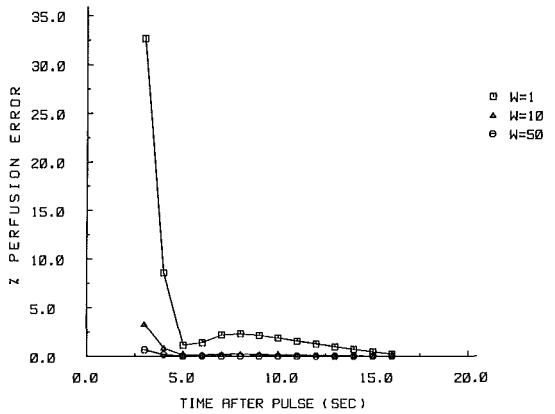

Fig. 9 Error of the SSM in perfusion predictions versus time after pulse using an effective radius of 0.3 mm for the solutions. Parameters used: $k = 0.5$ W/m°C, $\tau = 3$ seconds, $P = 5$ mW, and $R_{rm} = 0.15$ mm. W was varied from 1-50 kg/m^{3}s.

Discussion

For all of the conditions tested, the spherical source model more accurately predicted the local tissue perfusion and the thermal conductivity (results not shown) than the point source model, with significant decreases in error, especially for low blood perfusion situations. For example, the difference between the errors of each model ranged from 28 percent for a perfusion of 1 kg/m^{3}s to 1 percent for a perfusion of 50 kg/m^{3}s at a measurement time of 11 s after the pulse (a good measurement time) and all other parameters at their nominal values (Fig. 3).

All the prediction errors increase at shorter measurement times. At the short times, the error in the PSM is due to the fact that the thermistor has a finite size and therefore is not adequately modeled as a point source, as previously discussed by Arkin [6]. Similarly, the error in the SSM is due to the fact that the thermistor is surrounded by a passive coating of glass and epoxy and therefore is not a uniform power source such as assumed in the SSM. The longer measurement times ($t_m > 11$ seconds) produced acceptable results, within 10 percent for perfusions of 10 kg/m^{3}s or greater, but failed to adequately improve the predictions at lower flow rates. At these large measurement times the effective measurement volume of the probe has become large in comparison to the physical dimensions of the probe, and therefore the probe has begun to resemble a point source. Thus, both solutions become more accurate representations of the actual system and the predictions of the two models become similar. As suggested in Fig. 3, from the time where the errors approach a level less than approximately 10 percent and from the experimental protocol set up by Arkin, a measurement time interval centered at 11 seconds after the pulse was chosen as the ideal measurement time to be used in later simulations. Note that Arkin [5] determined that a measurement time interval from 6–12 seconds minimized the effects of experimentally derived errors. This time was found to be a trade off between too small of a measured temperature signal (experimentally derived errors) at long times and too large of a model error at the shorter times.

As noted previously, each of the models was used to simultaneously determine both the thermal conductivity and blood perfusion from the reference model temperature data. The accuracy of both models in predicting the simulated tissue thermal conductivity was always very good, with the spherical source solution consistently yielding slightly better results. In all cases the SSM estimations of thermal conductivity were a fraction of a percent closer than those of the PSM and all predictions from both models followed the same trends. The error decreased as the perfusion increased but was well below 2 percent in the time interval of interest. These accurate predictions are not unexpected, due to the conduction dominated nature of this technique [18].

The actual value of tissue (reference model) thermal conductivity was found to have a significant effect on the prediction of perfusion, as shown in Fig. 4. It is evident that larger values of tissue conductivity decrease the error in predicting perfusion. Again, the errors are larger at low values of perfusion (Fig. 5) and diminish as the measurement time is increased (results not shown). These effects are again a result of larger sampling volume obtained due to the increase in thermal conductivity which, for reasons mentioned previously, allow most of the bead properties to be neglected, and thus both model solutions become more accurate. To investigate the effect of several bead parameters, in particular the internal

bead thermal conductivity, specific heat, and density on the perfusion errors in both models, different test cases of the reference model were simulated, varying each parameter (results not shown). The internal composite conductivity values (from 1–15 W/m°C) have a negligible effect. Similarly, a +/− 50 percent change in the specific heat (from 835 J/kg°C) and density (from 2225 kg/m^3) of the composite was also found to have a negligible effect on the errors for the standard test conditions.

The effects of the pulse length on the prediction of various perfusion rates is shown in Fig. 5. This effect is most noticeable at low perfusion levels, where the shorter pulse lengths produce better results. For these shorter pulse lengths, the ratio of the measurement time (time after the pulse) to the pulse length is much greater, allowing for a large effective sensed volume at a shorter time. Again, making the finite bead results more closely approach the model predictions. At moderate to high perfusions the pulse length has little effect.

The physical dimensions of the thermistor bead (inner composite material, glass coating, and outer layer of epoxy) have an effect on the prediction errors (Fig. 6). Note the scale change between Figs. 6(a) and 6(b). Small deviations from the standard bead dimensions of 0.2 mm O.D. for the inner composite material, 0.25 mm O.D for the glass coating, and 0.3 mm O.D. for the epoxy layer caused a considerable change in error. An increase in the thickness of the epoxy layer from 0.3 mm to 0.4 mm O.D. increased the perfusion prediction error by 5–10 percent. Similarly, increasing the thickness of the glass coating to 0.35 mm O.D. and maintaining the epoxy layer at 0.4 mm O.D. increased the error another 5–10 percent. An increase of the inner composite material from 0.2 mm to 0.3 mm decreased the error by 5–10 percent. As the ratio of the outer diameter of the bead to the diameter of the inner resistive material is decreased, the thermistor is more closely approximated as a uniform power source which is an assumption in the derivation of both models. Also, as the outer diameter is decreased the thermistor geometry approaches that of a point source. The above analysis illustrates that the overall size and the internal composite diameter are significant bead properties in limiting prediction errors for both of the analytical models.

The effect of tissue trauma in the immediate volume surrounding the thermistor bead is shown in Fig. 7. The damaged region was modeled as a spherical annulus of tissue, without perfusion, surrounding the thermistor bead. For damage ranging in thickness from 0 to 3 bead radii, the effect on the resulting perfusion predictions was noticeably small for the SSM results.

Finally, turning to the results of Figs. 8 and 9, one can begin to answer the question, "Which SSM heated radius best models the actual bead performance?" Here one is free to choose any value for this radius between zero (which would reduce the SSM to the PSM, which the present study has shown to be a nonoptimal solution) and infinity. In the present study, we have used the physical dimension of the outer bead radius as the radius of the heated region of the SSM. This is a dimension which is easy to obtain experimentally, and reflects the fact that the thermistor bead is a physically separate entity of a given size immersed in the tissue. However, from the results of Fig. 8 it appears that there may be a better choice of the radius of the heated region in the SSM, a variable which we may call the "effective" bead radius. For the condition tested, it can be seen that the error approached zero for two effective radii; one was slightly less than the heated composite radius (0.1 mm) and the other was twice the actual outer bead radius. Choosing this latter radius of 0.3 mm as the effective radius, Fig. 9 illustrates how accurate the SSM can become when an optimal effective radius is used. By comparing Fig. 3 with Fig. 9 it is shown that the difference between using the effective radius and the actual physical radius in the SSM has a dramatic effect, especially at low blood flows. These results indicate that the size of the heated region in the SSM can be considered as an effective radius, and that perhaps probes can be calibrated to account for any inconsistencies between the SSM and the actual probe properties, allowing for more accurate determinations of perfusion and thermal conductivity. This concept of calibrating probes for effective properties is utilized in the implementation of the thermal diffusion probe method, a similar thermal clearance technique of determining perfusion that was developed by Bowman et al. [19–21]. The present study has concentrated on presenting the spherical source model and evaluating its performance when the effective bead radius (i.e., the size of the heated region in the SSM) equaled the actual outer bead radius. Further study is needed to determine under what conditions a better, optimal, choice of effective radius exists and the sensitivity of that choice to various parameters.

Clearly, from the above results, the spherical source model offers a better representation of the thermal pulse-decay process than that of the point source model. An obvious improvement in the pulse decay method would then be to replace existing PSM algorithms with the SSM algorithm. The amount of extra computation time, using Romberg numerical integration [13], would be small and the accuracy of the perfusion determination would be improved.

Conclusions

The spherical source model is more accurate than the point source model in describing the thermal decay process and consistently yields improved predictions for determining both the local tissue perfusion and thermal conductivity. For large measurement times and high perfusions these errors are limited to within 10 percent. For low blood flow, both models are inaccurate and produce errors in perfusion predictions in excess of 20–40 percent for the SSM and 30–50 percent for the PSM. These errors decrease with longer measurement times, shorter pulse lengths, and smaller bead diameters. The effect of tissue trauma within 3 bead radii of the probe is negligible. The accuracy of the SSM can be improved by allowing the heated source radius to be an effective value that is determined by a calibration of each probe. This process allows the SSM to predict perfusions in the 1–5 kg/m^{3}s range with errors less than 3 percent.

References

1 Chen, M. M., Holmes, K. R., and Rupinskas, V., "Pulse Decay Method for Measuring the Thermal Conductivity of Living Tissues," ASME JOURNAL OF BIOMECHANICAL ENGINEERING, Vol. 103, 1981, pp. 253–260.

2 Holmes, K. R., and Chen, M. M., "Local Tissue Heating: Microprobe Pulse-Decay Technique for Heat Transfer Parameter Evaluation," *Measurement of Blood Flow and Local Tissue Energy Production by Thermal Methods, Evaluation Methodology*, Muller-Schauenburg et al. (eds.), Thieme-Stratton Inc., New York, 1983, pp. 50–56.

3 Cheng, M. M., and Holmes, K. R., "Thermal Pulse-decay Method for Simultaneous Measurement of Thermal Conductivity and Local Blood Perfusion Rate of Living Tissues," *1980 Advances in Bioengineering*, V. C. Mow (ed.), American Society of Mechanical Engineers, New York, 1980, pp. 113–115.

4 Holmes, K. R., Arkin, H., Bottje, W. G., and Chen, M. M., "Thermal Pulse Decay Method for the Measurement of Local Tissue Blood Perfusion: A Validation Study," (personal communication).

5 Arkin, H., Holmes, K. R., and Chen, M. M., "A Sensitivity Analysis of the Thermal Pulse Decay Method for Measurement of Local Tissue Conductivity and Blood Perfusion," ASME JOURNAL OF BIOMECHANICAL ENGINEERING, Vol. 108, Feb. 1986, pp. 54–58.

6 Arkin, H., Holmes, K. R., Chen, M. M., and Bottje, W., "Thermal Pulse Decay Method for Simultaneous Measurement of Local Thermal Conductivity and Blood Perfusion: A Theoretical Analysis," ASME JOURNAL OF BIOMECHANICAL ENGINEERING, Vol. 108, No. 3, Aug. 1986, pp. 208–214.

7 Song, C. W., Lokshina, A., Rhee, J. G., Patten, M., and Levitt, S. H., "Implication of Blood Flow in Hyperthermic Treatment of Tumors," *IEEE Transactions on Biomedical Engineering*, Vol. BME-31, No. 1, Jan. 1984.

8 Eberhart, R. C., Shitzer, A., and Hernandez, E., "Thermal Dilution Methods: Estimation of Tissue Blood Flow and Metabolism," *Thermal Characteristics of Tumors: Applications in Detection and Treatment*, The New York Academy of Sciences, R. Jain and P. M. Gullino (eds.), New York, 1980, pp. 107–131.

9 Chato, J. C., "Measurement of Thermal Properties of Biological Materials," *Heat Transfer in Medicine and Biology*, Vol. One, A. Shitzer and R. C. Eberhart (eds.), Plenum Press, New York, 1985, pp. 167–192.

10 Goldenberg, H., "Heat Flow in an Infinite Medium Heated by a Sphere," *British J. Applied Physics*, Vol. 3, 1952, pp. 296–298.

11 Diederich, C. J., "The Implementation and Evaluation of Two Thermal Techniques for Measuring Local Tissue Perfusion," M.S. thesis, 1986, University of Arizona.

12 Roemer, R. B., "Heat Transfer in Hyperthermia Treatments: Basic Principles and Applications," *Biological, Physical, and Clinical Aspects of Hyperthermia*, B. Paliwal, F. Hetzel, M. Dewhirst (eds.), Am. Inst. of Physics, Inc., New York, NY, 1988, pp. 210–293.

13 Ferziger, J. H., *Numerical Methods for Engineering Application*, Wiley, 1981, pp. 32–40.

14 Sachse, H. B., *Semi-conducting Temperature Sensors and Their Applications*, Wiley, New York, 1975.

15 Incropera, F. P., and DeWitt, D. P., *Introduction to Heat Transfer*, Wiley, New York, 1985, p. 679.

16 Lee, H., and Neville, C., *Handbook of Epoxy Resin*, McGraw-Hill, 1982.

17 Beck, J. V., and Arnold, K. J., "Gauss Method of Minimization," *Parameter Estimation in Engineering and Science*, pp. 340–349, Wiley, New York, 1977.

18 Kress, R., and Roemer, R., "A Comparative Analysis of Thermal Blood Perfusion Measurement Techniques," ASME JOURNAL OF BIOMECHANICAL ENGINEERING, Vol. 109, 1987, pp. 218–225.

19 Balasubramaniam, T. A., and Bowman, H. F., "Thermal Conductivity and Thermal Diffusivity of Biomaterials: A Simultaneous Measurement Technique," ASME JOURNAL OF BIOMECHANICAL ENGINEERING, Vol. 99, 1977, pp. 148–154.

20 Bowman, H. F., Balasubramaniam, T. A., and Woods, M., "Determination of Tissue Perfusion From In Vivo Thermal Conductivity Measurements," ASME Winter Annual Meeting, Atlanta, Georgia, November 27–December 2, 1977.

21 Valvano, J., Allen, J., and Bowman,, H. F., "The Simultaneous Measurement of Thermal Conductivity, Thermal Diffusivity, and Perfusion in Small Volumes of Tissue," ASME JOURNAL OF BIOMECHANICAL ENGINEERING, Vol. 106, 1984, pp. 192–197.